Molecular & Biochemical Parasitology 202 (2015) 34–37

Contents lists available at ScienceDirect

Molecular & Biochemical Parasitology

Short technical report

Structural basis for the relaxed substrate selectivity of *Leishmania mexicana* broad specificity aminotransferase

Wen Jiang[a,b], Cristina Nowicki[c,**], Wulf Blankenfeldt[b,*]

[a] *Technische Universität Dortmund, Fakultät Chemie, Otto-Hahn-Str. 6, 44227 Dortmund, Germany*
[b] *Physical Biochemistry, Max Planck Institute for Molecular Physiology, Otto-Hahn-Str. 11, 44227 Dortmund, Germany*
[c] *IQUIFIB (CONICET-Facultad de Farmacia y Bioquímica, Universidad de Buenos Aires), Junín 956, 1113 Buenos Aires, Argentina*

ARTICLE INFO

Article history:
Received 5 May 2015
Received in revised form
29 September 2015
Accepted 30 September 2015
Available online 8 October 2015

Keywords:
Leishmaniasis
Metabolism
Transamination
Aminotransferase
Substrate specificity
Drug design

ABSTRACT

Leishmania species are early branching eukaryotic parasites that cause difficult-to-treat tissue-damaging diseases known as leishmaniases. As a hallmark of their parasitic lifestyle, *Leishmaniae* express a number of aminotransferases that are involved in important cellular processes and exhibit broader substrate specificity than their mammalian host's counterparts. Here, we have determined the crystal structure of the broad specificity aminotransferase from *Leishmania mexicana* (LmexBSAT) at 1.91 Å resolution. LmexBSAT is a homodimer and belongs to the α-branch of family-I aminotransferases. Despite the fact that the protein was crystallized in the absence of substrates and has lost the pyridoxal-5′-phosphate (PLP) cofactor during crystallization, the structure resembles the closed, ligand-bound form of related enzymes such as chicken cytosolic aspartate aminotransferase. Its broader substrate specificity seems to be rooted in increased flexibility of a substrate-binding arginine (R291) and the interactions of this residue with the N-terminus of the second chain of the dimer.

Leishmania are flagellated protozoan parasites that cause a broad spectrum of clinical manifestations in man, collectively referred to as leishmaniases. They are transmitted by phlebotomine sandflies, exposing more than 350 million people in tropical and subtropical countries at risk with an estimated 1.5–2 million new cases every year. No vaccines are available and current clinical treatments are unsatisfactory. In addition, *Leishmania* parasites frequently develop resistance, making the identification of new drug targets an urgent need [1].

Pathogenic protozoa like *Leishmania* spp. express aminotransferases that exhibit notably broader substrate specificities than their mammalian host counterparts [2,3]. This is also the case for the broad specificity aminotransferase from *Leishmania mexicana* (LmexBSAT, GenBank entry AF416601_1, UniProt entry Q71PB4; with the exception of a K412E mutation of the C-terminal residue, LmexBSAT is identical to TriTrypDB entry LmxM.34.0820). With respect to mammalian enzymes, LmexBSAT most closely resembles aspartate aminotransferases (ASATs; sequence identity approx. 45%), but other than the highly aspartate-specific ASATs, LmexBSAT displays the highest catalytic efficiencies when aromatic amino acids are transaminated with oxaloacetate as the amino acceptor. However, it also utilizes other substrate pairs, for instance aspartate or methionine with the 2-oxoacids 2-oxoglutarate, 2-oxoisocaproate and 2-oxomethiobutyrate [4,5].

Little is known about the source and fate of aromatic amino acids as well as about their intracellular concentration in *Leishmania* parasites. Berger et al. have postulated that aminotransferases that transaminate aromatic amino acids with 2-oxomethiobutyrate contribute to methionine regeneration in pathogenic protozoa, where methionine is utilized for polyamine biosynthesis [6]. Further, metabolic analysis using ^{13}C-labeled carbon sources in *in vitro* cultures have shown that *L. mexicana* promastigotes depend on anaplerotic reactions that produce 2-oxoglutarate. This 2-oxoacid is needed to synthetize glutamate, presumably because the uptake of this amino acid from the external milieu is very slow [7]. Glutamate is a precursor in pyrimidine [8], hexosamine [9] and, more importantly, trypanothione biosynthesis. Trypanothione is the major low molecular dithiol in these parasites and needs to be re-synthetized continuously because of its vital role in neutralizing oxidative stress resulting from the parasite's own metabolic activity as well as from the host immune response (for review see Ref. [10]).

* Corresponding author. Present address: Structure and Function of Proteins, Helmholtz Centre for Infection Research, Inhoffenstr. 7, 38124 Braunschweig, Germany.
** Corresponding author.
E-mail addresses: cnowicki@qb.ffyb.uba.ar (C. Nowicki), wulf.blankenfeldt@helmholtz-hzi.de (W. Blankenfeldt).

http://dx.doi.org/10.1016/j.molbiopara.2015.09.007
0166-6851/

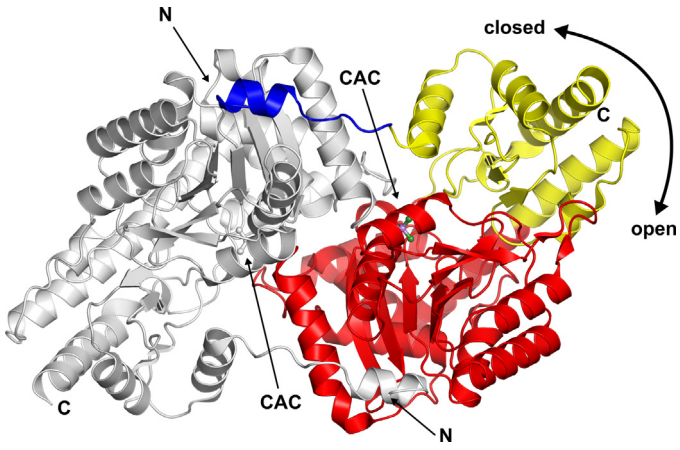

Fig. 1. Ribbon diagram of the LmexBSAT homodimer. One monomer is shown in grey, the other is colored according to domain structure (blue: N-terminal extension (M1–A20), yellow: substrate-binding domain (P21–Y54 & R328–E412), red: cofactor-binding domain (P55–E327). N- and C-termini are marked by N and C, respectively. Cacodylate ions (CAC) are shown as ball-and-stick models and indicate the position of the active sites. The colored monomer is in a slightly more closed conformation, which is a consequence of an inward rotation of the substrate-binding domain.

Table 1
Crystallographic details of LmexBSAT.

Data collection	
Wavelength (Å)	0.9763
Resolution range (Å)[a]	76.7–1.91 (1.94–1.91)
Space group	$P2_12_12_1$
Cell dimensions (a, b, c (Å))	86.41, 90.56, 142.16
Completeness (%)/multiplicity	99.3 (95.8)/4.5 (3.8)
Mean $I/\sigma(I)$	17.4 (2.1)
R_{merge}[b]	0.055 (0.629)
$R_{p.i.m.}$[c]	0.026 (0.365)
$CC_{1/2}$[d]	0.999 (0.649)
Overall B-factor from Wilson plot (A^2)	28
Refinement	
No. of reflections (R_{work}/R_{free})	82055/4344
R_{work}/R_{free}	0.177/0.210
No. of atoms protein/ions/water	6413/10/474
Average B-factors protein/ions/water (A^2)	41/58/43
r.m.s. deviations bond length (Å)/angles (°)	0.016/1.415
Ramachandran distribution (%)	
Favored/allowed/outliers	96.4/3.4/0.2
MolProbity score[e]	1.31

Recombinant LmexBSAT was produced in *E. coli* Rosetta2 pLysS cells and purified with standard methods. Initial crystallization conditions were determined by vapour diffusion in 24-well Linbro plates at 20 °C with hanging drops consisting of 1 μl precipitant and 1 μl protein solution (12 mg/ml in 20 mM Tris–HCl, 150 mM NaCl, pH 8.0) equilibrated against 500 μl reservoirs of the PACT and JCSG+ suites (Qiagen). After optimization, the precipitant consisted of 1 M tri-sodium citrate with 0.1 M sodium cacodylate buffer pH 6.0–7.0 at 12 °C. Crystals grew to a size of 30 × 30 × 70 μm (Fig. S1) and could be flash-cooled without further cryoprotection. Diffraction data were collected at 100 K on beamline X10SA of the Swiss Light Source (SLS, Paul Scherrer Institute, Villigen, Switzerland), integrated and pre-scaled with XDS [23] before post-scaling with AIMLESS [24]. Initial phases were obtained by molecular replacement with PHASER [25], using Protein Data Bank (PDB, [26]) entry 2CST [13] as a search model. Model building involved alternating rounds of manual adjustments in COOT [27] and maximum-likelihood refinement in phenix.refine [17]. For full details of experimental procedures refer to Supplemental data. Coordinates and structure factors have been deposited with PDB access code 4WB0.

[a] Values in parentheses refer to the highest resolution shell.

[b] $R_{merge} = \Sigma_{hkl}\Sigma_i|I_i(hkl) - \langle I(hkl)\rangle|/\Sigma_{hkl}\Sigma_i I_i(hkl)$, where $I_i(hkl)$ is the intensity of the *i*th observation of the reflection with index *hkl*.

[c] $R_{p.i.m.} = \Sigma_{hkl}\left\{1/[N(hkl)-1]\right\}^{1/2}\Sigma_i|I_i(hkl) - \langle I(hkl)\rangle|/\Sigma_{hkl}\Sigma_i I_i(hkl)$, where *N* is the number of observations of the reflections with index *hkl* [28].

[d] Pearson correlation coefficient [29].

[e] Score calculated by MolProbity [30].

While stage-specific changes in the energy metabolism of *Leishmania* are still poorly understood, recent data indicate that most enzymes involved in central carbon metabolism are constitutively expressed [11]. In line with this finding, proteomic analysis showed that LmexBSAT is expressed in amastigotes isolated from mammalian macrophages [12]. The enzyme is highly conserved in all sequenced *Leishmania* species (sequence identity 84–99%), but the respective genes have received the apparently false annotation as encoding putative ASATs.

A notable difference to mammalian ASATs is the observation that LmexBSAT catalyzes the transamination between aspartate and 2-oxoglutarate only in the forward direction, i.e. LmexBSAT is very inefficient in utilizing glutamate as an amino donor. This may hint at a role in supplying *Leishmania* with the essential building block glutamate. In order to understand differences to ASATs at the molecular level and to search for potential features that may be suitable for drug development, we have embarked in determining the crystal structure of LmexBSAT.

The enzyme was produced recombinantly and crystallized in spacegroup $P2_12_12_1$ with cell dimensions of 86.4, 90.6 and 142.2 Å. Diffraction data were collected to 1.91 Å resolution and molecular replacement positioned one dimer in the asymmetric unit, using a full atom model of chicken cytosolic aspartate aminotransferase (ChcASAT) in the closed conformation as search model (PDB entry 2CST [13], 43% sequence identity to LmexBSAT). With exception of a few residues from the N- and C-termini, both chains could be traced fully, and the model was refined to *R*-factors of R_{work} = 17.7 and R_{free} = 21.0% (Table 1).

LmexBSAT possesses a typical aminotransferase fold: each monomer consists of a smaller domain that contains the substrate binding residues (P21 to Y54 & R328 to the C-terminus at E412) into which a larger cofactor binding domain (P55 to E327) is inserted. The S-shaped dimer forms through interactions of the cofactor binding domains, and the first 20 N-terminal residues adopt an extended structure that inserts into a cleft formed on the cofactor binding domain of the other monomer (Fig. 1). The Cαs of both monomers superimpose with an rmsd of 0.74 Å, which is the consequence of a jaw-like movement of the small domain leading to a more closed conformation in monomer A. Similar open/closed transitions in other aminotransferases are associated with substrate binding [14], but since no ligands were observed here, the movement likely is induced by crystal packing effects.

The refined structure and the starting model 2CST superimpose with an rmsd of 1.22 Å in 791 of 809 Cα-positions. Other related structures were identified with PDBeFold [15], again confirming the high similarity to ASATs from vertebrate species. The most similar structure, however, is that of a putative aspartate aminotransferase from *Leishmania major* Friedlin (LmajASAT, PDB entry 4H51 [16]), which was not available when we first determined the structure of LmexBSAT. LmajASAT is 93% sequence-identical and superimposes with an rmsd of 0.71 Å in 800 of 801 Cα-positions.

Despite the fact that the purified recombinant LmexBSAT was yellow and active, crystals appeared colorless (Fig. S1) and only faint electron density for the cofactor pyridoxal-5′-phosphate (PLP) was observed towards the end of the refinement. Instead, the binding sites of PLP's phosphate group in both active sites were occupied with a cacodylate ion from the crystallization buffer (occupancy >90% after occupancy refinement in phenix.refine [17]), which was identified by anomalous density around the central atom (f″(As) = 3.35 e, f″(P) = 0.18 e, f″(S) = 0.23 e at the data collection wavelength of 0.9763 Å [18]; Fig. 2A). A similar loss of PLP was also observed during crystallization of LmajASAT, where cocrystallization with 2.5 mM PLP reinstalled the cofactor [16]. Because of the high sequence identity, the PLP-bound structure of LmajASAT

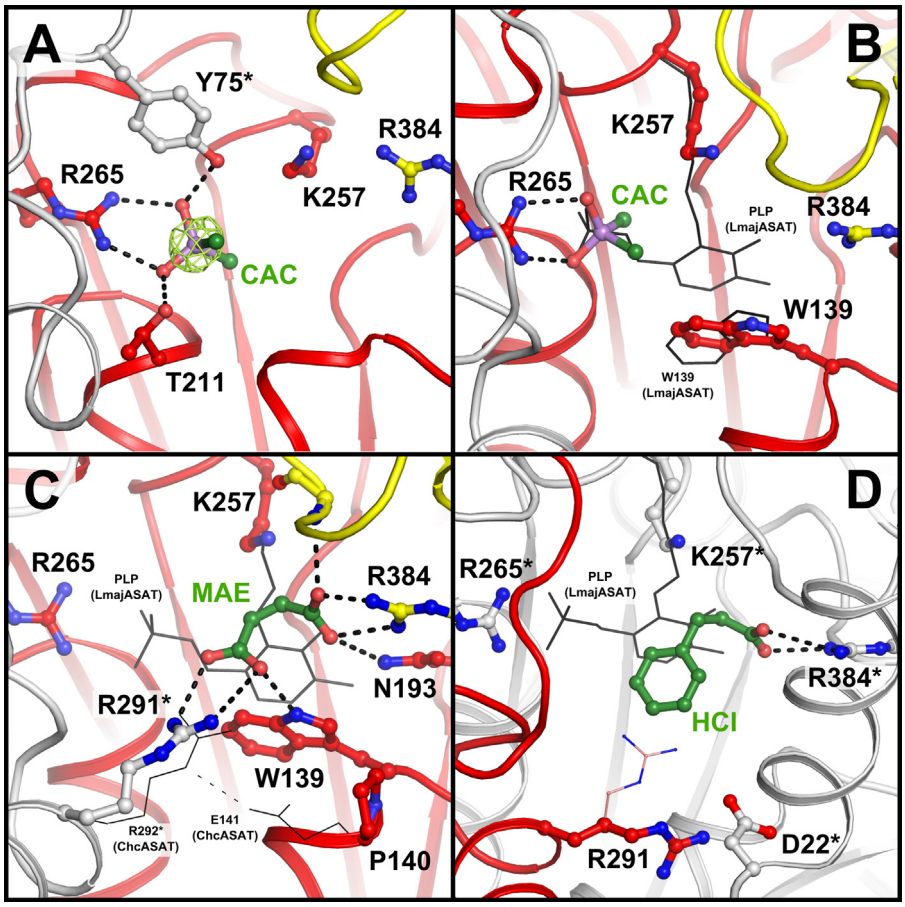

Fig. 2. Details of the active sites of LmexBSAT, shown from similar orientations. (A) Anomalous difference electron density around the arsenic atom of cacodylate (CAC) at 5 σ, calculated with phases from the final model and with diffraction data reported in Table 1. (B) Changes expected by binding of the cofactor pyridoxal-5′-phosphate PLP. Thin black lines indicate the position of PLP and of W139 in the closely related LmajASAT (PDB entry 4H51) [16]. (C) The superimposition of LmexBSAT with ChcASAT in complex with maleate (PDB entry 2CST; MAE: maleate; thin black lines show the position of PLP in LmajASAT and of E141 and R292* in ChcASAT as indicated) [13] explains why LmexBSAT prefers dicarboxylates with four carbon atoms chain length. (D) Flexibility of R291 indicates how aromatic substrates may be bound. The ligand 3-phenylpropionate has been placed by superimposition of the more open monomer of LmexBSAT with the respective complex of PdARAT (PDB entry 1AY8; HCI:3-phenylpropionate) [22]. Note that two conformations of R291 are only observed in the more open chain of LmexBSAT, hence the different tagging by * and the inverted colors with respect to panels A–C, for which the more closed chain was used. The smaller ball-and-stick model represents the inward conformation of R291, which would lead to unfavorable interactions with aromatic substrates.

provides a good reference point for deciphering changes that occur upon PLP binding in LmexBSAT. Superimposition reveals that the most prominent difference between the cofactor-free and cofactor-bound structure is a small repositioning and a rotation around the χ2 torsion angle of the sidechain of W139, which establishes a parallel π-stacking interaction between the indole moiety and the pyridine ring of PLP (Fig. 2B).

LmexBSAT belongs to the α-branch of family-I aminotransferases [5,19]. Based on substrate preferences, these enzymes fall into two groups, namely those which are specific for aspartate/oxaloacetate interconversion and those which accept a broader range of substrates including aromatic amino acids. Here, a ratio of k_{cat}/K_m for aspartate/2-oxoglutarate versus k_{cat}/K_m for phenylalanine/2-oxoglutarate of more than 1 indicates specificity for asparate. In an attempt to predict substrate specificity, Muratore et al. used amino acid conservation around the cofactor to identify ten subgroups within the Iα-subfamily and assessed substrate preference for one member of each subgroup [20]. This revealed that predictions are difficult because closely related subgroups showed opposite specificity. LmexBSAT belongs to subgroup 1, for which the authors investigated a cytosolic aspartate aminotransferase from *Trypanosoma brucei* (UniProt ID Q964F1). This enzyme was found to have a k_{cat}/K_m (Asp)/k_{cat}/K_m (Phe) of 0.49, in line with a value of 0.51 for similar substrates (aspartate/2-oxoglutarate versus phenylalanine/oxaloacetate) in LmexBSAT [5]. Even if no structure of a ligand complex of LmexBSAT or of another subgroup 1 aminotransferase is available, a comparison to complexes of other aminotransferases allows hypothesizing about determinants of the broad specificity observed in LmexBSAT. Here, ChcASAT in complex with maleate (PDB entry 2CST) [21] as representative of the aspartate-specific Iα-aminotransferases (subgroup 5), and *Paracoccus denitrificans* aromatic amino acid aminotransferase (PdARAT) in complex with 3-phenylpropionate (PDB entry 1AY8) [22] representing the broad specificity and aromatic aminotransferases (subgroup 2) are chosen (Fig. 2C/D). Superimposition shows that the active center of LmexBSAT contains two arginine residues to bind dicarboxylic amino acid derivatives, namely R291* and R384 (* indicating the other monomer). While R384 is responsible for establishing a salt bridge with the α-carboxylate group of the substrate, the less conserved R291* is involved in binding the substrate's side chain (Fig. 2C). In order to accommodate amino acids that are not acidic, R291* has to turn away to avoid electrostatic repulsion and to create space for larger substrates. Towards this end, it is instructive to investigate structures of PdARAT in complex with aromatic amino acid analogues such as 3-phenylpropionate (PDB entry 1AY8) [22]. Here, the arginine corresponding to R291* in LmexBSAT (R292*) has swung out of the active center to engage in a hydrogen bond with the backbone carbonyl of A13 (A20 in

LmexBSAT) and possibly also in an electrostatic interaction with the side chain of D15 (D22 in LmexBSAT). To establish these contacts, the N-terminal region containing these residues has moved towards the active center, similar to the transition to the more closed state observed in chain A of the crystal form of LmexBSAT described here (not shown). Therefore, similar outward displacement of R291* and relocation of the N-terminus may also occur in LmexBSAT, which is corroborated by the finding that the side chain of R291* is highly flexible and adopts at least one additional outward rotamer in the more open active center of chain B (Fig. 2D and Fig. S2). In the aspartate-specific ASATs, rotation of the corresponding arginine to an outward position may be hindered (R292* in ChcASAT). Here, the guanidino group seems anchored by a glutamic acid that is replaced by a proline in LmexBSAT and PdARAT (E141 in ChcASAT, P140 in LmexBSAT, P141 in PdARAT, Fig. 2C). It is thus tempting to hypothesize that the flexibility of arginine at position 291 determines whether a Iα-aminotransferase is specific for aspartate or is able to utilize aromatic amino acids as well.

Interestingly, LmexBSAT shows only weak activity towards glutamate (app. k_{cat} 16.1 s^{-1}; app. k_{cat}/K_m 0.09 mM^{-1} s^{-1} in the glutamate/oxaloacetate combination) [4], which may be linked to the finding that the unliganded and therefore likely open conformation of LmexBSAT most closely resembles the closed, ligand-bound form of other aminotransferases, as was also noted for LmajASAT [16]. This is exemplified by superimposition with the maleate complex of ChcASAT (PDB entry 2CST). Here, the carboxylates of the C4-molecule maleate from ChcASAT align perfectly to salt-bridge with R291 and R364* of LmexBSAT, indicating that binding a C5-moiety may be difficult (Fig. 2C). However, these steric restraints are obviously relaxed for the second half reaction of LmexBSAT (regeneration of PLP from pyridoxamine-5′-phosphate PMP), since decent k_{cat} and k_{cat}/K_m values are obtained when 2-oxoglutarate is used as a second substrate (app. k_{cat} 192 s^{-1}; app. k_{cat}/K_m 70 mM^{-1} s^{-1} for aspartate in the aspartate/2-oxoglutarate combination) [4]. Apparently, PMP provides the active site with more flexibility to accommodate the larger 2-oxoglutarate, which may allow LmexBSAT to act in supplying glutamate to the parasite.

In summary, the crystal structure described here suggests that flexibility of R291 reduces substrate selectivity and allows the turnover of aromatic amino acids by LmexBSAT. Further, the observation that ligand-free LmexBSAT resembles the closed conformation of other aminotransferases explains the higher activity with aspartate than with glutamate. Together, these structural properties reflect the parasitic lifestyle of *Leishmania* species and their need to preserve glutamate as a precursor for the generation of key molecules such as trypanothione.

Acknowledgements

The authors are grateful to Roger S. Goody for hosting this project at the Max Planck Institute for Molecular Physiology in Dortmund, Germany. The use of beamtime and the support by beamline staff of the Swiss Light Source at the Paul Scherrer Institute in Villigen, Switzerland, is gratefully acknowledged. CN was supported by the DAAD-UBA exchange program.

Appendix A. Supplementary data

Supplementary data associated with this article can be found, in the online version, at http://dx.doi.org/10.1016/j.molbiopara.2015.09.007.

References

[1] S.L. Croft, P. Olliaro, Leishmaniasis chemotherapy–challenges and opportunities, Clin. Microbiol. Infect. 17 (2011) 1478–1483.
[2] D. Marciano, C. Llorente, D.A. Maugeri, C. de la Fuente, F. Opperdoes, J.J. Cazzulo, et al., Biochemical characterization of stage-specific isoforms of aspartate aminotransferases from *Trypanosoma cruzi* and *Trypanosoma brucei*, Mol. Biochem. Parasitol. 161 (2008) 12–20.
[3] D. Marciano, D.A. Maugeri, J.J. Cazzulo, C. Nowicki, Functional characterization of stage-specific aminotransferases from trypanosomatids, Mol. Biochem. Parasitol. 166 (2009) 172–182.
[4] J. Vernal, J.J. Cazzulo, C. Nowicki, Isolation and partial characterization of a broad specificity aminotransferase from *Leishmania mexicana* promastigotes, Mol. Biochem. Parasitol. 96 (1998) 83–92.
[5] J. Vernal, J. José Cazzulo, C. Nowicki, Cloning and heterologous expression of a broad specificity aminotransferase of *Leishmania mexicana* promastigotes, FEMS Microbiol. Lett. 229 (2003) 217–222.
[6] L.C. Berger, J. Wilson, P. Wood, B.J. Berger, Methionine regeneration and aspartate aminotransferase in parasitic protozoa, J. Bacteriol. 183 (2001) 4421–4434.
[7] E.C. Saunders, W.W. Ng, J.M. Chambers, M. Ng, T. Naderer, J.O. Krömer, et al., Isotopomer profiling of Leishmania mexicana promastigotes reveals important roles for succinate fermentation and aspartate uptake in tricarboxylic acid cycle (TCA) anaplerosis, glutamate synthesis, and growth, J. Biol. Chem. 286 (2011) 27706–27717.
[8] N.S. Carter, P. Yates, C.S. Arendt, J.M. Boitz, B. Ullman, Purine and pyrimidine metabolism in *Leishmania*, Adv. Exp. Med. Biol. 625 (2008) 141–154.
[9] T. Naderer, E. Wee, M.J. McConville, Role of hexosamine biosynthesis in *Leishmania* growth and virulence, Mol. Microbiol. 69 (2008) 858–869.
[10] R.L. Krauth-Siegel, M.A. Comini, Redox control in trypanosomatids, parasitic protozoa with trypanothione-based thiol metabolism, Biochim. Biophys. Acta 1780 (2008) 1236–1248.
[11] K. Leifso, G. Cohen-Freue, N. Dogra, A. Murray, W.R. McMaster, Genomic and proteomic expression analysis of *Leishmania* promastigote and amastigote life stages: the *Leishmania* genome is constitutively expressed, Mol. Biochem. Parasitol. 152 (2007) 35–46.
[12] D. Paape, M.E. Barrios-Llerena, T. Le Bihan, L. Mackay, T. Aebischer, Gel free analysis of the proteome of intracellular *Leishmania mexicana*, Mol. Biochem. Parasitol. 169 (2010) 108–114.
[13] V.N. Malashkevich, B.V. Strokopytov, V.V. Borisov, Z. Dauter, K.S. Wilson, Y.M. Torchinsky, Crystal structure of the closed form of chicken cytosolic aspartate aminotransferase at 1.9 A resolution, J. Mol. Biol. 247 (1995) 111–124.
[14] A.C. Eliot, J.F. Kirsch, Pyridoxal phosphate enzymes: mechanistic, structural, and evolutionary considerations, Annu. Rev. Biochem. 73 (2004) 383–415.
[15] E. Krissinel, K. Henrick, Secondary-structure matching (SSM), a new tool for fast protein structure alignment in three dimensions, Acta Crystallogr. D: Biol. Crystallogr. 60 (2004) 2256–2268.
[16] J. Abendroth, R. Choi, A. Wall, M.C. Clifton, C.M. Lukacs, B.L. Staker, et al., Structures of aspartate aminotransferases from *Trypanosoma brucei*, *Leishmania major* and *Giardia lamblia*, Acta Crystallogr. F: Struct. Biol. Commun. 71 (2015) 566–571.
[17] P.D. Adams, P.V. Afonine, G. Bunkóczi, V.B. Chen, I.W. Davis, N. Echols, et al., PHENIX: a comprehensive Python-based system for macromolecular structure solution, Acta Crystallogr. D: Biol. Crystallogr. 66 (2010) 213–221.
[18] S. Sasaki, Numerical Tables of Anomalous Scattering Factors Calculated by the Cromer and Liberman's Method. KEK Rep 88-14, 1989, pp. 1–136.
[19] R.A. Jensen, W. Gu, Evolutionary recruitment of biochemically specialized subdivisions of Family I within the protein superfamily of aminotransferases, J. Bacteriol. 178 (1996) 2161–2171.
[20] K.E. Muratore, B.E. Engelhardt, J.R. Srouji, M.I. Jordan, S.E. Brenner, J.F. Kirsch, Molecular function prediction for a family exhibiting evolutionary tendencies toward substrate specificity swapping: recurrence of tyrosine aminotransferase activity in the Iα subfamily, Proteins 81 (2013) 1593–1609.
[21] S. Rhee, M.M. Silva, C.C. Hyde, P.H. Rogers, C.M. Metzler, D.E. Metzler, et al., Refinement and comparisons of the crystal structures of pig cytosolic aspartate aminotransferase and its complex with 2-methylaspartate, J. Biol. Chem. 272 (1997) 17293–17302.
[22] A. Okamoto, Y. Nakai, H. Hayashi, K. Hirotsu, H. Kagamiyama, Crystal structures of *Paracoccus denitrificans* aromatic amino acid aminotransferase: a substrate recognition site constructed by rearrangement of hydrogen bond network, J. Mol. Biol. 280 (1998) 443–461.
[23] W. Kabsch, XDS, Acta Crystallogr. D: Biol. Crystallogr. 66 (2010) 125–132.
[24] P.R. Evans, G.N. Murshudov, How good are my data and what is the resolution? Acta Crystallogr. D: Biol. Crystallogr. 69 (2013) 1204–1214.
[25] A.J. McCoy, R.W. Grosse-Kunstleve, P.D. Adams, M.D. Winn, L.C. Storoni, R.J. Read, Phaser crystallographic software, J. Appl. Crystallogr. 40 (2007) 658–674.
[26] H.M. Berman, J. Westbrook, Z. Feng, G. Gilliland, T.N. Bhat, H. Weissig, et al., The Protein Data Bank, Nucleic Acids Res. 28 (2000) 235–242.
[27] P. Emsley, B. Lohkamp, W.G. Scott, K. Cowtan, Features and development of Coot, Acta Crystallogr. D: Biol. Crystallogr. 66 (2010) 486–501.
[28] M.S. Weiss, Global indicators of X-ray data quality, J. Appl. Crystallogr. 34 (2001) 130–135.
[29] P.A. Karplus, K. Diederichs, Linking crystallographic model and data quality, Science 336 (2012) 1030–1033.
[30] V.B. Chen, W.B. Arendall, J.J. Headd, D.A. Keedy, R.M. Immormino, G.J. Kapral, et al., MolProbity: all-atom structure validation for macromolecular crystallography, Acta Crystallogr. D: Biol. Crystallogr. 66 (2010) 12–21.